Optical-absorption studies on noncubic s^2 centers in single crystals of KH_2PO_4 and RbH_2PO_4

Ikuo Fujita
Department of Physics, Faculty of Engineering, Shizuoka University, Johoku 3-5-1, Hamamatsu, Shizuoka 432, Japan
(Received 2 July 1993)

Effects of a noncubic crystal field on the s^2 ion are investigated. Optical-absorption spectra of thallous ion centers produced in single crystals of KH_2PO_4 (KDP) and RbH_2PO_4 (RDP) are presented. They consist of polarized absorption bands. Since it is confirmed that the Tl^+ centers in KDP and RDP exhibit quite similar absorption characteristics, a model is proposed to interpret the interaction mechanisms between the s^2 ions and the KDP-like crystal lattices. Among five typical absorption bands named A_z, A_{xy}, B_{xy}, C_{xy}, and C_z, the A_{xy} band has a noticeable doublet structure and the B_{xy} band is as intense as the A_{xy} band even at liquid-nitrogen temperature and is strongly temperature dependent. The observed results are qualitatively explained by taking into account the spin-orbit, crystal-field, and electronic-vibrational interactions.

I. INTRODUCTION

Marked progress in experimental techniques and methods of analysis has been made in understanding the electronic properties of point imperfections in crystalline solids and their interactions with host lattices. Among various kinds of point defects, impurity ions with s^2 electronic configuration introduced into alkali halide crystals have been one of the most attractive objects of physical research.[1,2]

Alkali halide crystals are extremely suitable for experimental and theoretical studies of the s^2 centers. They are fairly well-understood crystals with cubic lattices and their outstanding transparency in a wide range from infrared to vacuum ultraviolet, where the so-called A, B, and C absorption bands due to the s^2 ions appear, makes optical measurements feasible. Accordingly alkali halides have extensively been adopted as host crystals. Impurity ions embedded in the crystals take the places of alkali-metal ions and the symmetry of the crystal field at the impurity site is the highest point symmetry O_h. Many experiments, in which external perturbations such as mechanical stress,[3-5] electric,[6] and magnetic[7-9] fields were utilized to produce noncubic environments around the s^2 centers, have been conducted to obtain further information to determine the physical parameters of experimental and theoretical interest.

It is rather difficult to find noncubic host crystals where the s^2 centers exhibit a number of uv absorption bands which allow study of the various interactions between the impurity ion and the host lattice. A unique case is potassium dihydrogen phosphate (KDP) doped with thallous ions, KH_2PO_4:Tl (KDP:Tl).[10] Some other studies have been carried out on s^2 centers in noncubic lattices,[11,12] but the Tl^+ center in KDP:Tl is so far the only s^2 center in a noncubic host lattice where all the possible $s^2 \rightarrow sp$ transitions corresponding to the A, B, and C bands in alkali halides have been confirmed.

The present work was undertaken to observe optical absorption of Tl^+ centers in thallium-doped rubidium dihydrogen phosphate single crystals RbH_2PO_4:Tl (RDP:Tl) and to study the general absorption characteristics of s^2 ion centers in the KDP-like lattices. Each of the Tl^+ ions in these crystals occupies an alkali-ion site whose local symmetry is lower than that of the similar center in alkali halide crystals. One naturally expects that absorption bands in those systems exhibit crystal-field-allowed components and certain polarization characteristics. It is confirmed that such absorptions exist in the expected photon-energy range not only in KDP:Tl, but also in RDP:Tl. The fact that the integrated absorption intensity of a crystal-field-allowed band increases as temperature rises demonstrates cooperative contribution of the spin-orbit and electron-lattice interactions to the intensity. It is shown that the observed spectra in these systems can be explained qualitatively by a simple model in terms of the spin-orbit, crystal-field, and vibronic ion-lattice interactions.

II. EXPERIMENTAL METHOD

Host crystals were grown from supersaturated aqueous solutions and the recrystallization technique was adopted to improve the crystal quality by reducing impurities.[13,14] Thallium ions were added to the solution of the purified crystals in the form of TlCl (99.9% pure), but the chlorine ions existing in the solution did not seem to affect the crystal growth. Furthermore, a comparison of optical absorption of KDP grown in a KCl-doped solution with that of KDP grown in an undoped solution did not indicate any trace of additional absorption due to KCl in the spectral range of our interest. X- and z-cut sample plates of each crystal were prepared to measure absorption spectra polarized in parallel and perpendicular to the z axis of the crystal.

A vacuum monochromator equipped with a 50-cm concave grating and a hydrogen-arc discharge tube as a light source was used since most absorption measurements were made in the vacuum uv region. Its spectral resolution was about 0.4 nm. Plane-polarized light was obtained by use of a polarizer made of two parallel LiF

0163-1829/94/49(10)/6462(8)/$06.00

plates which reflected incident light at the Brewster angle. The polarizer was placed between the light source and the entrance slit of the monochromator and was made rotatable together with the light source to attain an arbitrary direction of polarization. The spectral resolution in this instance was about 1.6 nm due to inevitable decrease of light intensity at the LiF polarizer. Two recording spectrophotometers, a Cary model 14 and a Shimadzu model UV-2100, were also utilized for absorption measurements of z-cut samples with unpolarized light only in the spectral range above 190 nm.

III. uv ABSORPTION SPECTRA

Absorption of the Tl-doped crystals rises at about 5 eV in photon energy and the spectra give several band peaks toward higher energy up to the fundamental absorption tail of each crystal. Polarization-dependent spectra in KDP:Tl and RDP:Tl measured at room temperature (RT) and at liquid-nitrogen temperature (LNT) are shown in Figs. 1 and 2. The spectra are decomposed into individual component bands termed A_z, A_{xy}, B_{xy}, C_{xy}, and C_z. The symbol A_z, for example, stands for an absorption band corresponding to the A band of Tl^+ centers in alkali halides and to its polarization parallel to the z axis of the host crystal. Anisotropy in the plane perpendicular to the z axis was not noticed in the A_{xy}, B_{xy}, and C_{xy} bands. This isotropy provided the advantage that the xy components, in particular a doublet structure noticed in the A_{xy} band, could be measured by use of z-cut sample plates and intense unpolarized light, which led to optimal spectral resolution.

In KDP:Tl five absorption bands were seen at LNT, but the C_z band and a large portion of the C_{xy} band were concealed by the fundamental absorption of the host crystal at RT. In RDP:Tl, on the other hand, only four absorption bands, whose general features are quite similar to those in KDP:Tl, were observed. Though one might expect a C_z band in the vicinity of the strong C_{xy} band, it could not be distinguished from the strong host absorption.

Positions, full widths at half maximum (FWHM), and intensities of the absorption bands at RT and LNT are summarized in Table I. The intensities are obtained as integrated absorption coefficients relative to the A_z band area of each crystal at LNT. The values in parentheses stand for the doublet components of the A_{xy} band, which is decomposed into two Gaussian subbands by numerical approximation.

Intensities of the A_z, A_{xy}, and B_{xy} bands at LNT are nearly equal in both crystals, while the C_{xy} and C_z bands are very intense in comparison with the first three bands. The intensity of the B_{xy} band at RT is larger than at

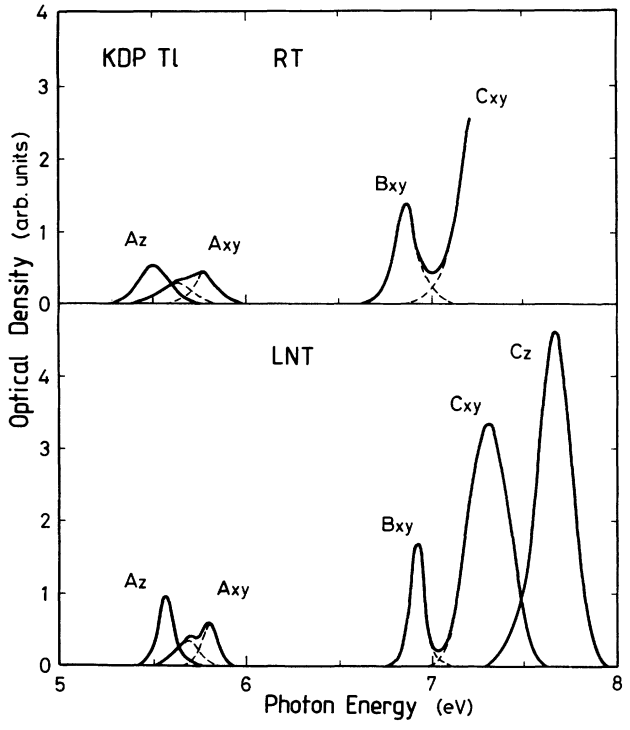

FIG. 1. Polarized absorption bands in KDP:Tl measured at RT and LNT. The label A_z, for example, signifies that the band corresponds to the A band in the Tl^+ center in alkali halides and the polarization of the light absorbed is parallel to the z axis of the crystal. All the expected absorption bands corresponding to the $s^2 \rightarrow sp$ transitions in S_4 symmetry are seen. Dashed curves represent approximate decompositions of the overlapping bands.

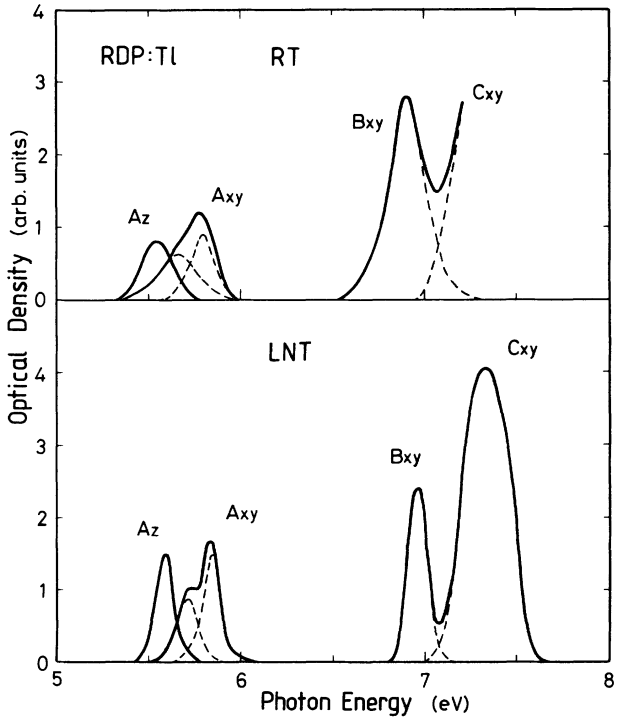

FIG. 2. Absorption bands in RDP:Tl at RT and LNT. General features are very similar to those of KDP:Tl but the intensity change in the B_{xy} band is rather enhanced. A doublet structure is clearly seen in the A_{xy} band. The peak position of the C_{xy} band at RT was not confirmed due to the strong fundamental absorption of RDP. The ordinate scales in Figs. 1 and 2 are independent.

TABLE I. Positions, FWHM's, and intensity ratios of the absorption bands in KDP:Tl and RDP:Tl measured at RT and LNT. The intensity ratio of each band is determined as the integrated absorption strength of the band relative to that of the A_z band at LNT. Values in parentheses stand for the doublet components of the A_{xy} band.

	Absorption band		A_z	A_{xy}	B_{xy}	C_{xy}	C_z
KDP:Tl	Position (eV)	RT	5.53	5.73(5.63,5.78)	6.88		
		LNT	5.56	5.76(5.68,5.81)	6.91	7.30	7.67
	FWHM (eV)	RT	0.21	(0.20,0.16)	0.19		
		LNT	0.10	(0.14,0.12)	0.09	0.26	0.22
	Intensity ratio	RT	1.00	1.28(0.59,0.69)	2.35		
		LNT	1.00	1.22(0.56,0.66)	1.85	8.0	9.8
RDP:Tl	Position (eV)	RT	5.55	5.72(5.64,5.80)	6.90		
		LNT	5.58	5.80(5.72,5.84)	6.96	7.35	
	FWHM (eV)	RT	0.21	(0.26,0.16)	0.2		
		LNT	0.12	(0.18,0.10)	0.12	0.34	
	Intensity ratio	RT	0.80	1.48(0.74,0.74)	3.6		
		LNT	1.00	1.62(0.76,0.86)	1.7	6.9	

LNT. Note that in RDP:Tl the B_{xy} band at RT becomes about twice as intense as at LNT. The fundamental absorption tail of each crystal prevents precise measurements of intensity changes in the C_{xy} and C_z bands.

IV. DESCRIPTION OF THE MODEL

A theoretical model to interpret optical spectra of the s^2 impurity centers in solids was proposed by Seitz.[15] In this model an s^2 ion substituted at a cation site exhibits essentially the same electronic transitions as those of the free ion, and the lattice environment causes a phonon-assisted transition and broadening of the optical spectra. Various improvements have been made on the model describing interactions between the impurity ion and the surrounding ions: the Jahn-Teller distortions play an important role in explaining rather complicated structures in the observed absorption[16] and emission[17,18] spectra, the molecular-orbital approach revealed an interaction mechanism between the central ion and the ligand ions,[19–21] an integration method in multidimensional space was developed to calculate band shapes,[22] and the method of moments[23] was applied to estimate physical parameters from band shapes.[24]

In the case of alkali halides the nondegenerate s^2 ground state of these impurity ions is $^1S_0$ ($^1A_{1g}$ of O_h symmetry) and the first excited state is a twelvefold-degenerate sp state which splits into the following multiplets: $^3P_0$ ($^3A_{1u}$), $^3P_1$ ($^3T_{1u}$), $^3P_2$ ($^3T_{2u}$,^3E_u), and $^1P_1$ ($^1T_{1u}$). Three absorption bands called A, B, and C, whose energies are characteristic to each impurity-host combination, are commonly observed. The $^1A_{1g}\rightarrow{}^3T_{1u}$ transition allowed by the spin-orbit interaction gives the A band. The $^1A_{1g}\rightarrow(^3T_{2u},^3E_u)$ transition assigned to the B band is allowed only by vibrational mixing of $^3T_{2u}$ and/or ^3E_u with $^3T_{1u}$ in addition to the spin-orbit coupling. Naturally the B band intensity is very weak at low temperatures and increases gradually as temperature rises. The transition $^1A_{1g}\rightarrow{}^1T_{1u}$ is allowed by the electric dipole and spin selection rules, yielding the most intense C band. These bands have temperature-dependent structures which are understood in terms of the spin-orbit interaction and the vibronic interaction.

KDP:Tl and RDP:Tl exhibit quite similar absorption spectra where the A_z, A_{xy}, B_{xy}, and C_{xy} bands are confirmed in common. We should note two obvious differences between these spectra and those of thallous ion centers in alkali halides, i.e., anisotropy of the absorption and large intensity of the B_{xy} band, which indicate the importance of the crystal field around the Tl^+ center in understanding the spectra of KDP:Tl and RDP:Tl.

The host crystals undergo ferroelectric phase transitions at 123 K in KDP and at 147 K in RDP.[25] The crystal lattice being tetragonal in the paraelectric phase above the transition temperature T_c and orthorhombic in the ferroelectric phase below T_c, the exact symmetry of the K^+ or Rb^+ site is lowered at the transition to the ferroelectric phase.[26] The influence of the transition was clearly observed as small changes in the positions and shapes of the bands.[27] However, approximate local symmetry around a Tl^+ ion may be estimated by reference to the well-known crystal structure of KDP in the paraelectric phase[28] at any temperature of our interest, because no drastic changes, disregarding the finer details such as the peak shifts mentioned above, were observed in the absorption spectra in spite of the phase transition.

This point of view has been set forth in the interpretation of a number of polarized absorption bands observed in the KDP:Tl spectra.[10] The absorption spectra of RDP:Tl seem to support the idea and to give impetus to the attempt to describe a model with explicit expressions of the interactions, which would be useful for analysis of the s^2 centers in KDP-like lattices. Inspection of the interaction matrices constructed in the present work, for instance, will elucidate mutual location of the bands and the magnitude of the crystal-field splitting between the A_{xy} and A_z bands relative to that between the C_{xy} and C_z bands.

When a thallous ion introduced in these crystals replaces an alkali-metal ion, it is surrounded by four first-

neighbor and four second-neighbor oxygen ions as shown in Fig. 3. These eight oxygen ions are considered to exert the most important part of the crystal field upon the central ion. The point symmetry of the local field is then S_4 as a good approximation. The possible lower-symmetry field existing in the ferroelectric phase is considered to be much weaker than the S_4 field.

The Hamiltonian of our model is expressed as follows:

$$\mathbf{H}=\mathbf{H}_{\text{free}}+\mathbf{H}_{\text{SO}}+\mathbf{H}_{\text{cryst}}+\mathbf{H}_{\text{vibronic}} ,$$

where $\mathbf{H}_{\text{free}}$ represents the free-ion Hamiltonian without the spin-orbit interaction $\mathbf{H}_{\text{SO}}$, $\mathbf{H}_{\text{cryst}}$ the static crystal-field energy, and $\mathbf{H}_{\text{vibronic}}$ the electron-vibrational interaction between Tl^+ and neighboring ions. To the accuracy of the present analysis, $\mathbf{H}_{\text{cryst}}$ can be written as $\mathbf{H}'_{\text{cryst}}+\mathbf{H}_{\text{C}}$ where $\mathbf{H}'_{\text{cryst}}$ is the largest part of the static field of almost spherical symmetry and $\mathbf{H}_{\text{C}}$ is the S_4 field proportional to $2z^2-x^2-y^2$, ignoring weak fields of lower symmetry. The simplest form of $\mathbf{H}_{\text{vibronic}}$ leads to linear dependence of the interaction energy on the vibrational-mode coordinate Q and is denoted by $\mathbf{H}_{\text{Q}}$. The Hamiltonian may now be rewritten as

$$\mathbf{H}=\mathbf{H}_0+\mathbf{H}_{\text{SO}}+\mathbf{H}_{\text{C}}+\mathbf{H}_{\text{Q}} ,$$

where $\mathbf{H}_0=\mathbf{H}_{\text{free}}+\mathbf{H}'_{\text{cryst}}$. The last three terms $\mathbf{H}_{\text{SO}}$, $\mathbf{H}_{\text{C}}$, and $\mathbf{H}_{\text{Q}}$ are treated as perturbations to $\mathbf{H}_0$.

In order to compare the Tl^+ center in the KDP lattice with that in the cubic alkali halide lattice, a set of wave functions which diagonalize $\mathbf{H}_0$ are grouped according to the irreducible representations of two point groups O_h and S_4. The ground-state electronic configuration of Tl^+ is s^2 and the wave function ϕ_0 with singlet spin multiplicity belongs to the totally symmetric representation A_{1g} of O_h in the cubic environment, and likewise it belongs to the representation A of S_4 in the S_4 field. Twelve wave functions for the first excited sp configuration are given in Table II with irreducible representations of O_h and S_4 symmetries.

The interaction Hamiltonian $\mathbf{H}_0+\mathbf{H}_{\text{SO}}+\mathbf{H}_{\text{C}}$ is given in Table III, neglecting the Madelung potential and Coulomb integral. We see that the spin-orbit interaction ζ mixes the singlet states ϕ_1,ϕ_2,ϕ_3 and triplet states $\phi_9,\phi_{10},\phi_{11}$ and that the crystal-field interaction D combines two singlet states ϕ_1,ϕ_2 with the triplet states ϕ_4,ϕ_5 by way of the spin-orbit interaction.[29]

An interaction matrix of $\mathbf{H}_{\text{Q}}$ is constructed to consider some temperature-dependent phenomena observed in the absorption spectra. Vibrational modes of the thallous ion and the eight ligand oxygen ions forming S_4 symmetry can be treated as three interaction modes with four interaction-mode coordinates.[30] They are a totally symmetric A-mode coordinate Q_1, a B-mode coordinate Q_2, and two E-mode coordinates Q_3 and Q_4. In Table IV the matrix is given in the linear approximation where the interaction is described as

$$\mathbf{H}_{\text{Q}}=\sum_{i=1}^{4}\mathbf{V}_i Q_i .$$

The coefficient $\mathbf{V}_i$ is a function of the coordinates of the electrons derived as the first derivative of $\mathbf{H}_{\text{vibronic}}$ with respect to Q_i.

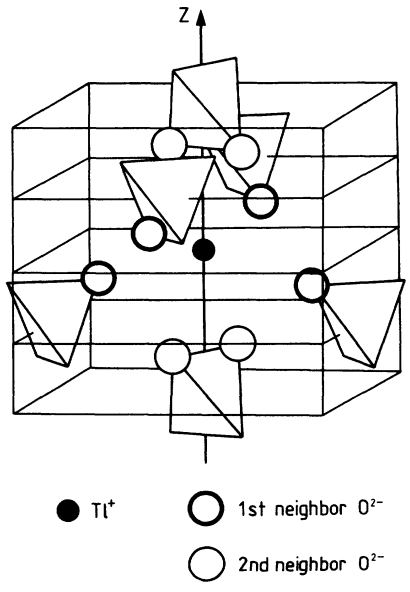

FIG. 3. Perspective view of the Tl^+ center in KDP. A Tl^+ ion at the center is surrounded by six PO_4 tetrahedra. Two of them, located immediately above and below the Tl^+ ion along the crystal z axis, provide four second-neighbor oxygen ions. Four first-neighbor oxygen ions belong to the remaining four tetrahedra. The symmetry of the center is then S_4.

TABLE II. The sp wave functions and their associated irreducible representations (IR) of O_h and S_4 symmetries with spin multiplicities. U_0 and (U_x,U_y,U_z) stand for the singlet and the triplet spin functions of the two-electron system and (X_0,Y_0,Z_0) and (X,Y,Z) for the symmetric and antisymmetric orbital functions, respectively. The orbital functions are $X_0=\{s(1)p_x(2)+s(2)p_x(1)\}/\sqrt{2}$, $X=\{s(1)p_x(2)-s(2)p_x(1)\}/\sqrt{2}$, etc., where $s(1)$ and $p_x(2)$ are one-electron orbital functions of electron 1 in the s state and of electron 2 in the p_x state, respectively.

IR of O_h	Wave function	IR of S_4
$^1T_{1u}$	$\phi_1=U_0X_0$	^1E
	$\phi_2=U_0Y_0$	
	$\phi_3=U_0Z_0$	^1B
$^3T_{2u}$	$\phi_4=(U_yZ+U_zY)/\sqrt{2}$	^3E
	$\phi_5=(U_zX+U_xZ)/\sqrt{2}$	
	$\phi_6=(U_xY+U_yX)/\sqrt{2}$	^3A
^3E_u	$\phi_7=(U_xX-U_yY)/\sqrt{2}$	^3A
	$\phi_8=(2U_zZ-U_xX-U_yY)/\sqrt{6}$	^3B
$^3T_{1u}$	$\phi_9=i(U_yZ-U_zY)/\sqrt{2}$	^3E
	$\phi_{10}=i(U_zX-U_xZ)/\sqrt{2}$	
	$\phi_{11}=i(U_xY-U_yX)/\sqrt{2}$	^3B
$^3A_{1u}$	$\phi_{12}=(U_xX+U_yY+U_zZ)/\sqrt{3}$	^3B

TABLE III. Energy matrix including the spin-orbit interaction $\mathbf{H}_{SO}$ and the crystal-field interaction $\mathbf{H}_C$. G: exchange interaction (Coulomb interaction is neglected); ζ: spin-orbit interaction; λ: King and Van Vleck's parameter considering the difference between singlet and triplet radial functions (Ref. 29); and D: crystal-field interaction, $D \equiv (\langle X|\mathbf{H}_C|X\rangle + \langle Z|\mathbf{H}_C|Z\rangle)/2$.

ϕ_1	ϕ_2	ϕ_3	ϕ_4	ϕ_5	ϕ_6	ϕ_7	ϕ_8	ϕ_9	ϕ_{10}	ϕ_{11}	ϕ_{12}
$G-2D$	0	0	0	0	0	0	0	$\lambda\zeta/\sqrt{2}$	0	0	0
	$G-2D$	0	0	0	0	0	0	0	$\lambda\zeta/\sqrt{2}$	0	0
		$G+4D$	0	0	0	0	0	0	0	$\lambda\zeta/\sqrt{2}$	0
			$-G+\zeta/2+D$	0	0	0	0	$3iD$	0	0	0
				$-G+\zeta/2+D$	0	0	0	0	$-3iD$	0	0
					$-G+\zeta/2-2D$	0	0	0	0	0	0
						$-G+\zeta/2-2D$	0	0	0	0	0
							$-G+\zeta/2+2D$	0	0	0	$2\sqrt{2}D$
			*					$-G-\zeta/2+D$	0	0	0
									$-G-\zeta/2+D$	0	0
										$-G-\zeta/2-2D$	0
											$-G-\zeta$

TABLE IV. Matrix of the linear vibrational interaction $\mathbf{H}_Q = \sum_i \mathbf{V}_i Q_i$ $(i=1,2,3,4)$. Q's are the interaction-mode coordinates and a, b, c, and d the coupling constants defined as follows: $a \equiv \langle X|\mathbf{V}_1|X\rangle$, $b \equiv \langle Z|\mathbf{V}_1|Z\rangle$, $c \equiv \langle X|\mathbf{V}_2|Y\rangle$, and $d \equiv \langle Y|\mathbf{V}_3|Z\rangle = \langle Z|\mathbf{V}_4|X\rangle$.

ϕ_1	ϕ_2	ϕ_3	ϕ_4	ϕ_5	ϕ_6	ϕ_7	ϕ_8	ϕ_9	ϕ_{10}	ϕ_{11}	ϕ_{12}
aQ_1	cQ_2	dQ_4	0	0	0	0	0	0	0	0	0
	aQ_1	dQ_3	0	0	0	0	0	0	0	0	0
		bQ_1	0	0	0	0	0	0	0	0	0
			$4(a+b)Q_1/2$	$cQ_2/2$	$dQ_4/2$	$-dQ_3/2$	$\sqrt{3}dQ_3/3$	$-i(a-b)Q_1/2$	$icQ_2/2$	$-idQ_4/2$	$\sqrt{6}dQ_3/3$
				$(a+b)Q_1/2$	$dQ_3/2$	$dQ_4/2$	0	$-icQ_2/2$	$i(a-b)Q_1/2$	$idQ_3/2$	$\sqrt{6}dQ_4/3$
					0	0	$-\sqrt{3}cQ_2/3$	$idQ_4/2$	$-idQ_3/2$	0	$\sqrt{6}cQ_2/3$
						0	0	$-idQ_3/2$	$-idQ_4/2$	icQ_2	0
							$-(a-2b)Q_1/3$	$i\sqrt{3}dQ_3/3$	$i\sqrt{3}dQ_4/2$	0	$-\sqrt{2}(a-b)Q_1/3$
			*					$(a+b)Q_1/2$	$cQ_2/2$	$dQ_4/2$	0
									$(a+b)Q_1/2$	$dQ_3/2$	0
										aQ_1	0
											$(2a+b)Q_1/3$

V. DISCUSSION

The spin-orbit interaction $\mathbf{H}_{SO}$ and the crystal-field interaction $\mathbf{H}_C$ not only resolve the degeneracy in O_h symmetry but also mix the states ϕ's. $\mathbf{H}_C$ in particular, as seen in Table II, splits the threefold-degenerate states into a twofold-degenerate state and a nondegenerate state ($T_{1u} \rightarrow E + B$ and $T_{2u} \rightarrow E + A$), and the twofold-degenerate state into two nondegenerate states ($E_u \rightarrow A + B$).

A schematic energy diagram to illustrate level splittings of the *sp* configuration by the exchange energy G, the spin-orbit interaction ζ, and the crystal-field interaction D is shown in Fig. 4, where energy shifts due to the Madelung energy and Coulomb integral are not shown. Although values of the energy parameters G, ζ, λ, and D are unknown, the diagram is tentatively constructed with the relation $\zeta \approx 2D \gg D$. The value of G smaller than ζ is not so unreasonable, because considerable reduction of G has been obtained experimentally and confirmed by theoretical study on the Tl^+ centers in alkali halides.[20,31,32] A relatively small value is used for D because of the small crystal-field splitting between the A_{xy} and A_z bands in comparison with the splitting by the spin-orbit interaction. Effects of mixing among the eigenstates of $\mathbf{H}_0$ due to the off-diagonal elements are not shown, except the singlet-triplet mixing by the spin-orbit interaction.

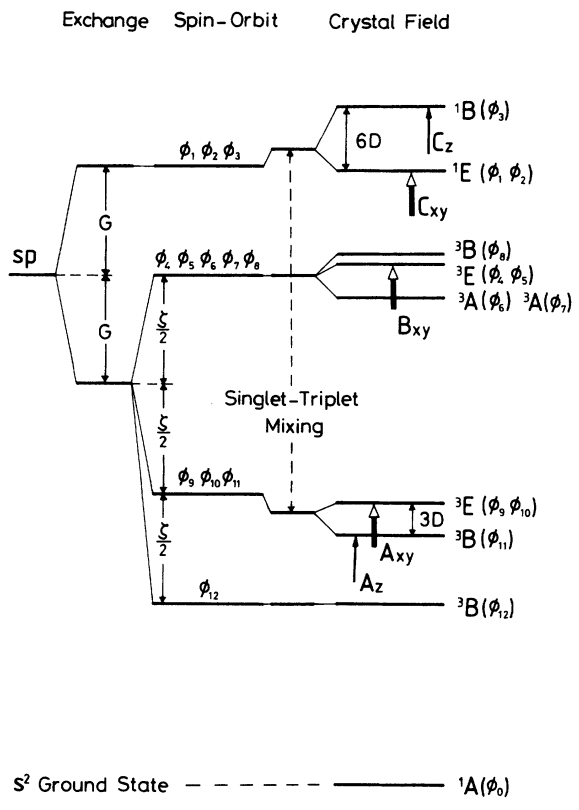

FIG. 4. Schematic energy diagram showing splittings of the twelvefold-degenerate *sp* state with respect to the exchange interaction G, the spin-orbit interaction ζ, and the crystal-field interaction D. Repulsion between the $^1T_{1u}$ and $^3T_{1u}$ levels due to the spin-orbit interaction is also shown. At the extreme right, energy levels in the S_4 crystal fields are shown with the corresponding wave functions given in Table II. The two kinds of arrows indicate the allowed transitions of different polarizations from the s^2 ground state and are labeled with the corresponding absorption bands observed.

By diagonalizing the interaction matrix, mixed eigenstates are obtained in the form of linear combinations among the singlet and triplet states. The mixed states may hereafter be designated by the same notations (ϕ's) without confusion.

Mixing between three doubly degenerate states $E(\phi_1,\phi_2)$, $E(\phi_4,\phi_5)$, and $E(\phi_9,\phi_{10})$ gives three new doubly degenerate states, each of which shares the spin-singlet state $E(\phi_1,\phi_2)$. Three electric dipole transitions from the spin-singlet s^2 ground state $^1A(\phi_0)$ are allowed, to result in the corresponding absorption bands $A_{xy}(\phi_0 \rightarrow \phi_9\phi_{10})$, $B_{xy}(\phi_0 \rightarrow \phi_4,\phi_5)$, and $C_{xy}(\phi_0 \rightarrow \phi_1,\phi_2)$, with polarization perpendicular to the z axis of the crystal. The B_{xy} band is allowed by cooperation of the spin-orbit and crystal-field interactions.

The $^1B(\phi_3)$ and $^3B(\phi_{11})$ states also combine to give new ϕ_3 and ϕ_{11} which allow the C_z absorption ($\phi_0 \rightarrow \phi_3$) and the A_z absorption ($\phi_0 \rightarrow \phi_{11}$), respectively, for light polarized parallel to the z axis. Another mixing occurs between two triplet states ϕ_8 and ϕ_{12} but it is trivial in the present absorption experiment.

Consequently five electric dipole transitions indicated by arrows in Fig. 4 are possible from the ground state $^1A(\phi_0)$. Two $A \rightarrow B$ transitions correspond to the A_z and C_z bands and three $A \rightarrow E$ transitions to the A_{xy}, B_{xy}, and C_{xy} bands.

Diagonal elements of the matrix in Table III indicate that the crystal-field interaction locates $^1B(\phi_3)$ at the higher-energy side of $^1E(\phi_1,\phi_2)$ by $6D$ and $^3B(\phi_{11})$ at the lower-energy side of $^3E(\phi_9,\phi_{10})$ by $3D$, as shown in Fig. 4. This is just the order of the observed bands. If the mixing by the crystal field is not so large, the energy difference between the C_{xy} and C_z bands should be larger than that between the A_{xy} and A_z bands by a factor of about 2. In the present study the factor is calculated from the values in Table I to be $(7.67-7.30)/(5.76-5.56)=1.85$ in KDP:Tl at LNT, although much more detailed analysis may be required for quantitative comparison.

The doublet structure of the A_{xy} band can be explained by the vibrational interaction $\mathbf{H}_Q$. The matrix clarifies that the B interaction mode Q_2 combines the two states belonging to any doubly degenerate E representation. The doublet structure, however, is not observed in the B_{xy} and C_{xy} bands. This difference may be ascribed to the strength of the interaction, which should be estimated by the spatial extent of the electronic wave functions and by those of the ligand ions. Among the three E states, the electron charge distribution of the state $^3E(\phi_9,\phi_{10})$ extends along the z axis[33] toward four second-neighbor oxygen ions closely situated along the z axis. In addition, the interaction coordinate Q_2 includes displacement of the thallous ion along the z axis, which is directly connected with the ferroelectric modes[34-36] derived from the

KDP lattice structure. The displacement leads to closer contact between the electrons of the thallous ion and those of the four second-neighbor oxygen ions. This seems to be the most probable reason why the A_{xy} band exhibits the obvious doublet structure. Since the FWHM of the C_{xy} band is rather large it might have some vibronic structure. The existence of strong fundamental absorption in the host crystals KDP and RDP, however, prevents accurate measurements of their exact shapes at various temperatures.

The magnitude of the peak separation of the doublet component bands has been closely investigated in KDP:Tl between 4.2 and 346 K.[27] Although a rather complicated behavior is observed around the transition temperature T_c, it is almost unchanged between 4.2 K and T_c. Therefore, the origin of the structure below T_c seems to be of static nature. On the other hand, the separation above T_c increases as temperature rises. Since the separation is proportional to the square root of the temperature, the structure is ascribed to the dynamical Jahn-Teller effect of the $A \rightarrow E$ transition[37] which results from interaction between the twofold-degenerate electronic state $E(\phi_4,\phi_5)$ and the B-mode vibrations.

The oscillator strengths of the five absorption bands in KDP:Tl have been determined.[38] The value for the B_{xy} band is 0.10 at LNT and increases as temperature rises. This value is five to ten times larger than that of the B band of the s^2 centers in alkali halides.[16,39] The fact that the B_{xy} band in KDP:Tl as well as in RDP:Tl is as intense as the A_{xy} band even at LNT means that contribution of the S_4 crystal field to the B_{xy} band intensity should be comparable to that of the spin-orbit interaction.

The temperature dependence of the B_{xy} band intensity can naturally be attributed to the vibrational interaction. It is recognized by reference to the matrix $\mathbf{H}_Q$ that the totally symmetric vibrational mode Q_1 contributes to the B_{xy} band intensity just like the S_4 crystal field. The B mode Q_2 also couples (ϕ_4,ϕ_5) with (ϕ_9,ϕ_{10}). These interactions cause intensity transfer among the A_{xy}, B_{xy}, and C_{xy} bands.

In KDP:Tl net intensity transfer occurs from the C_{xy} band to the B_{xy} band, because the A_{xy} band intensity is almost unchanged. Possible intensity change in the C_{xy} band could not be confirmed within the experimental accuracy limited by strong superposition of the host absorption. In RDP:Tl a remarkable increase of the B_{xy} band intensity seems to be attained at the cost of the A_{xy} and C_{xy} band intensities. Since one-half of the B_{xy} band intensity in RDP:Tl at RT is the temperature-dependent increase, contribution of the vibrational interaction $\mathbf{H}_Q$ to the B_{xy} band intensity is of equal importance to the spin-orbit and crystal field interactions, $\mathbf{H}_{SO}$ and $\mathbf{H}_C$.

Intensity distributions between the two component bands of the A_{xy} band are rather approximate because of arbitrariness in the method of decomposition. It may be stated, however, that the A_{xy} band consists of two subbands with nearly equal strength in both KDP:Tl and RDP:Tl.

ACKNOWLEDGMENTS

The author wishes to thank Yoshihiro Miwa and Toshiyuki Suzuki for their assistance in the early stage of this work.

[1]W. B. Fowler, in *Physics of Color Centers,* edited by W. B. Fowler (Academic, New York, 1968), Chap. 2.
[2]Y. Farge and M. P. Fontana, *Electronic and Vibrational Properties of Point Defects in Ionic Crystals* (North-Holland, Amsterdam, 1979), Chaps. 3 and 4.
[3]D. Bimberg, W. Dultz, and K. Fussgaenger, Phys. Lett. **25A**, 766 (1967).
[4]D. Bimberg, W. Dultz, and W. Gebhardt, Phys. Status Solidi **31**, 661 (1969).
[5]T. Shimada and M. Ishiguro, Phys. Rev. **187**, 1089 (1969).
[6]A. Ranfagni, G. P. Fazzi, P. Fabeni, M. Bacci, M. P. Fontana, and G. Viliani, Phys. Rev. Lett. **35**, 753 (1975).
[7]R. Onaka, T. Mabuchi, and A. Yoshikawa, J. Phys. Soc. Jpn. **58**, 1036 (1967).
[8]M. P. Fontana and J. A. Davis, Phys. Rev. Lett. **23**, 974 (1969).
[9]V. Grasso, P. Perillo, and G. Vermiglio, Solid State Phys. **11**, 563 (1972).
[10]I. Fujita, J. Phys. Soc. Jpn. **44**, 257 (1978).
[11]A. Wolfert and G. Blasse, J. Lumin. **33**, 213 (1985).
[12]H. Abe and T. Mabuchi, J. Phys. Soc. Jpn. **56**, 276 (1986).
[13]G. M. Loiacono, Ferroelectrics **5**, 101 (1973).
[14]V. I. Bespalov, V. I. Bredikhin, V. P. Ershov, V. I. Katsman, and S. Yu. Potapenko, Growth Cryst. (USSR) **17**, 123 (1991).
[15]F. Seitz, J. Chem. Phys. **6**, 150 (1938).
[16]A. Fukuda, Sci. Light (Tokyo) **13**, 64 (1964).
[17]R. S. Knox and D. L. Dexter, Phys. Rev. **104**, 1245 (1956).
[18]A. Fukuda, S. Makishima, T. Mabuchi, and R. Onaka, J. Chem. Phys. Solids **28**, 1763 (1967).
[19]S. Sugano, J. Chem. Phys. **36**, 122 (1962).
[20]S. Sakoda and T. Tsuboi, Phys. Rev. B **22**, 4966 (1980).
[21]A. Ranfagni, D. Mugnai, M. Bacci, M. Montagna, O. Pilla, and G. Viliani, Phys. Rev. B **20**, 5358 (1979).
[22]K. Cho, J. Phys. Soc. Jpn. **27**, 646 (1969).
[23]C. H. Henry, S. E. Schnatterly, and C. P. Slichter, Phys. Rev. **137**, A583 (1965).
[24]A. Honma, J. Phys. Soc. Jpn. **24**, 1082 (1968).
[25]F. Jona and G. Shirane, *Ferroelectric Crystals* (Pergamon, Oxford, 1962), p. 87.
[26]T. Mitsui *et al.*, in *Ferroelectrics and Related Substances,* edited by K.-H. Hellwege and A. M. Hellwege, Landolt-Börnstein, New Series, Group III, Vol. 16, Pt. b (Springer-Verlag, New York, 1982), p.69.
[27]I. Fujita, J. Phys. Soc. Jpn. **46**, 1889 (1979).
[28]W. Känzig, in *Solid State Physics: Advances in Research and Applications,* edited by F. Seitz and D. Turnbull (Academic, New York, 1957), Vol. 4, p. 150.
[29]G. W. King and J. H. Van Vleck, Phys. Rev. **56**, 464 (1939).
[30]Y. Toyozawa and M. Inoue, J. Phys. Soc. Jpn. **21**, 1663 (1966).
[31]H. Kamimura and S. Sugano, J. Phys. Soc. Jpn. **14**, 1612 (1959).
[32]D. Bramanti, M. Mancini, and A. Ranfagni, Phys. Rev. B **3**, 3670 (1971).

[33]A. M. Lemos, M. C. Stauber, and J. F. Marion, Phys. Rev. B **2**, 4161 (1970).
[34]W. Cochran, Adv. Phys. **10**, 401 (1961).
[35]M. S. Shur, Kristallografiya **11**, 448 (1966) [Sov. Phys. Crystallogr. **11**, 394 (1966)].
[36]J. Skalyo, Jr., B. C. Frazer, and G. Shirane, Phys. Rev. B **1**, 278 (1970).
[37]M. D. Sturge, in *Solid State Physics: Advances in Research and Applications,* edited by F. Seitz and D. Turnbull (Academic, New York, 1957), Vol. 20, p. 191.
[38]I. Fujita, T. Suzuki, and Y. Miwa, J. Phys. Soc. Jpn. **51**, 3998 (1982).
[39]W. Wagner, Z. Phys. **181**, 143 (1964).